JOURNAL OF OPTOELECTRONICS AND ADVANCED MATERIALS Vol. 9, No. 3, March 2007, p. 587 - 590

Atomic environment changes in titanium-hydroxyapatite sintered powders induced by mechanical strain

V. SIMON[a*], D. LAZĂR[a], C. POPA[b], A. F. TAKÁCS[c], M. NEUMANN[c], S. SIMON[a]
[a]*Babes-Bolyai University, Faculty of Physics, 400084 Cluj-Napoca, Romania*
[b]*Technical University of Cluj-Napoca, Faculty of Materials Science and Engineering, Cluj-Napoca 400020, Romania*
[c]*University of Osnabrück, Physics Department, 49069 Osnabrück, Germany*

The effects of mechanical strains induced in titanium-hydroxyapatite sintered powders compressed under different pressures are investigated using X-ray photoelectron and electron spin resonance spectroscopic data. New cationic sites with modified electronic charge densities are evidenced. Hydroxyl species which increase the surface ability for self-assembly of nanoscale hydroxyapatite like structures on endosseous implants are evidenced on the surface of samples compressed at higher pressure.

(Received November 15, 2006; accepted December 21, 2006)

Keywords: Titanium-hydroxyapatite, Mechanical strain, Oxygen vacancy, XPS, EPR

1. Introduction

Surface coating with hydroxyapatite (HA), a crystalline form of calcium phosphate, is the common way to improve the biocompatibility of orthopaedic and dental titanium-based materials [1]. HA is both biocompatible and bioactive material, however, due to its poor mechanical properties and design limitations is not suitable for applications as a load bearing implant. This could be overcome by using appropriate metallic enforcer with hydroxyapatite [2]. One key problem is to produce implant surfaces with the ability to nucleate HA in the body fluid. Functionally graded materials consisting of metallic and ceramic components can attract improved properties of several systems such as medical implant devices [3]. There are different techniques of producing HA appropriate for these purposes. Sol-gel technology offers an alternative technique for producing hydroxyapatite for enhanced bone attachment [4, 5]. The bone attachment depends to a great extent on the material surface.

X-ray photoelectron spectroscopy (XPS) gives quantitative information on the elemental composition of a surface and the local chemical environment of the atoms comprising the surface [6]. Electron paramagnetic resonance (EPR) spectroscopy is one of the most efficient methods for the characterization of local order in structurally disordered systems [7].

The purpose of this work is to study changes induced by mechanical strain in the electronic structure and implicitly in the local order in titanium-hydroxyapatite sintered powders compressed under different pressures using X-ray photoelectron and electron spin resonance spectroscopic data.

2. Experimental

Titanium powder containing 0.01% Fe; 0.01% Al; 0.001% Si; 0.05% Mg impurities and hydroxyapatite prepared through a sol-gel technique were used to prepare samples with 5 weight % hydroxyapatite. Powders were pressed by applying forces of 30 and 35 kN in a rigid die with the surface of 0.5 cm^2, without the use of any lubricant. The pressed pellets were subsequently vacuum sintered (10^{-6} Torr) at 1160 °C for 60 minutes, with dwelling stages at 200, 600 and 800°C. The bulk density of the sintered samples was determined using Archimedes method. X-ray diffraction analysis (DRX) was carried out on powder and sintered samples using a Bruker Avance diffractometer.

XPS measurements were performed using a PHI 5600ci Multi Technique system with monochromatised Al K_α radiation from a 250 W X-ray source ($h\nu$ = 1486.6 eV). During the measurements the pressure in the analysis chamber was in the 10^{-9} Torr range. High resolution core level scans were acquired for the C 1s, Ti 2p, Ca 2p, P 2p and O 1s photoelectron peaks. The absolute binding energies of the photoelectron spectra were determined by referencing to the C1s transition at 284.6 eV originating most probably during the measurements from adsorbed species. The position and full width at half maximum of photoelectron peaks were determined using spectrum simulation based on summation of Lorentzian and Gaussian functions.

Electron spin resonance analysis was carried out on powder samples with an ADANI spectrometer, at room temperature, in the X band (9.4 GHz) with 4 G modulation amplitude.

3. Results and discussion

The density of the samples sintered under 30 kN is 3.08 g/cm^3 and for those sintered under 35 kN is 3.19 g/cm^3. The composition at the sample surfaces was determinated from the XPS survey spectra. The ratio between calcium and phosphorus is around 2.5 and not 1.67 like in HA powder, but the accuracy of this value can be affected by the low precision in phosphorous determination due to its very low atomic concentration in the samples. The oxygen content exceeds 50 at % in both sets of samples and can be explained by oxidation during the sintering process, even though neither TiO_2, TiO nor Ti_2O crystalline species [1, 8, 9] are evidenced in XRD patterns.

The diffraction pattern recorded from the hydroxyapatite powder used for sintering is shown in Fig. 1a and contains the principal diffraction peaks of HA [10] which appear at 2θ values of 25.9º, 31.9º (triplet) and at 34.0º. The crystal size estimated from diffractograms using the Scherrer formula [11] is around 8 nm. After sintering 95Ti-5HA composite samples, only a titanium metallic phase is identified [12] in the XRD patterns of the obtained samples (Fig. 1b and 1c). The absence of any lines associated with hydroxyapatite type phases points out that after sintering these phases are highly distorded or/and partially vitrified. The titanium metallic phase seems to consist in crystals preferentially oriented to the sample surface, depending on the sintering pressure.

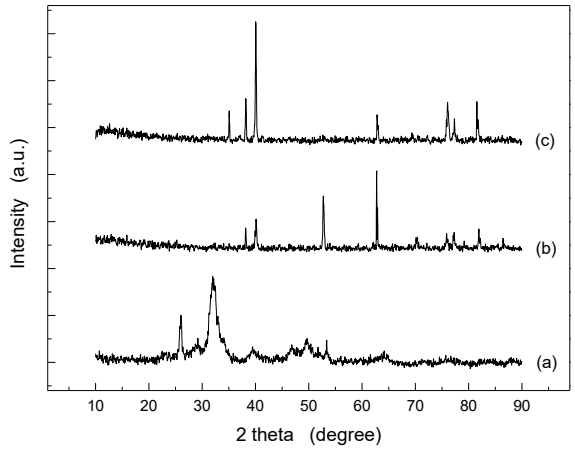

Fig. 1. XRD patterns of the (a) HA powder used for sintering, (b) sintered sample compressed under 600 MPa (c) sintered sample compressed under 700 MPa.

The Ti 2p core level photoelectron spectra practically do not differ for the two sets of samples (Fig. 2), while in the Ca 2p core level photoelectron spectra (Fig. 3) one can recognise a shift to higher binding energies and the occurrence of new cationic sites with increasing powder compression. The strains induced by applying a higher pressure are sufficient to cause the calcium cations charge changes. This, in turn, results in the electronic properties also being modified. The XPS technique is highly surface sensitive due to the short range of the escape depth of the photoelectrons that are excited in the solid, nevertheless it has been shown that the XPS spectra of samples are sensitive to the built-in strain [13]. The information offered by XPS spectra should be capable to distinguish several environments of the elements present in the investigated sample [14-16].

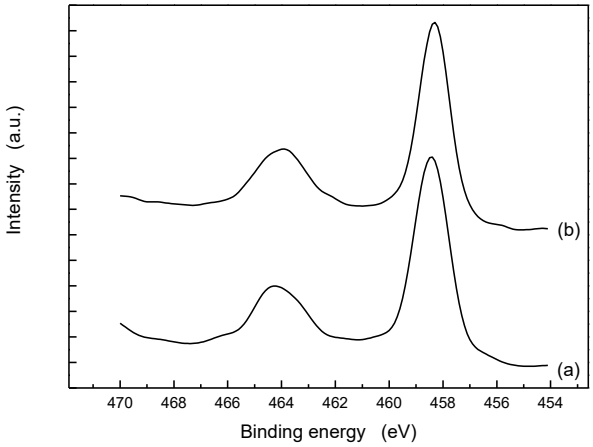

Fig. 2. Ti 2p core level photoelectron spectra of (a) sample compressed under 600 MPa (b) sample compressed under 700 MPa.

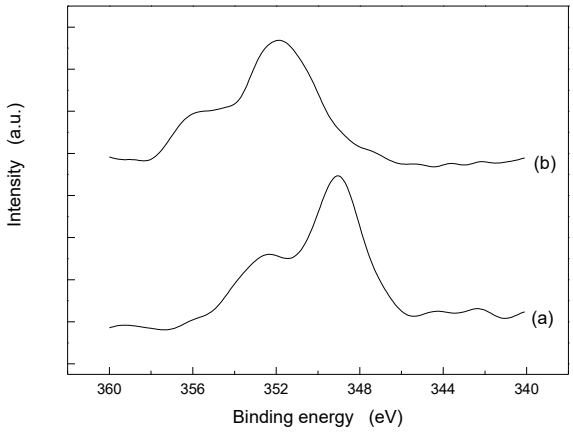

Fig. 3. Ca 2p core level photoelectron spectra of (a) sample compressed under 600 Mpa (b) sample compressed under 700 MPa.

Spin-orbit splitting leads to $2p_{1/2}$ and $2p_{3/2}$ peaks in Ti 2p and Ca 2p core level photoelectron spectra. Titanium is found to be involved in a dominant fraction as Ti^{4+}, as evidenced by the Ti $2p_{3/2}$ photoelectron peak close to 459.0 eV, with a spin-orbit splitting of 5.7 eV. The higher binding energies denote a decrease in effective electronic charge density around the atoms, but the large shift, around 3 eV, observed for calcium cations when the compression pressure is 700 Mpa, is more likely related to charged particles, probably calcium oxide or phosphate, occurring on the surface of the sample. It can be deduced that the extrinsic Ca^{2+} ions will capture oxygen, which gives rise to oxygen vacancies [17].

The problem to provide implant surfaces with the ability to nucleate HA from body fluid and implicitly from an aqueous solution is of special interest for endosseous implants. Despite major developments in prosthetic technologies, implants often fail because of an inadequate direct bone-to-implant interface (osseointegration) [18, 19]. The self-assembly of nanoscale structures like hydroxyapatite is used to mimic the natural biomineralization process to create the hardest tissue in the human body [20]. An enhanced HA nucleation can be achieved by *(i)* functionalized surfaces acting as molecular blueprints for site-directed nucleation, *(ii)* elevated supersaturation of HA at the surface, and *(iii)* surface topography providing confined reaction microenvironments and geometrically matched nucleating sites. This can be related to the generation of a hydroxylated surface with Ti–OH groups acting as nucleating sites for HA. The O 1s core level spectra can indicate the occurrence of OH bonds. The oxide-bound species O^{2-} are related to binding energies close to 530.0 eV and hydroxide-bound species OH^- are recorded close to 531.3 eV [21].

Fig. 4 shows the XPS peaks for O 1s which clearly indicate at least two oxygen-related surface components characterised by different binding energies. The O 1s core level spectrum of the samples compressed under 600 MPa (Fig. 4a) consits of two peaks corresponding to 529.95 and 533.05 eV, which shows the presence of two types of oxygen [21-23]. The higher binding energy peak dominates in this sample. The O 1s core level spectrum of the sample compressed under 700 MPa is pronouncedly modified (Fig. 4b). An increase in electron density at the oxygen atoms leads to lower electron binding energies. The component at low binding energy, 529.80 eV, is prevalent and that at higher binding energy is well fitted with two components, at 531.10 and 532.60 eV. An additional photoelectron peak is recorded at 535.95 eV and might be related to charged calcium oxide or phosphate particles. The signal at 531.1 eV is assigned to OH^- species, that at 532.60 eV can be assigned to O^{2-} ions in oxygen deficient regions [17, 24]. The binding energy corresponding to the new photoelectron peak is shifted with about 3 eV to higher BE values. The same shift was observed in Ca 2p photoelectron spectra. The fraction of the differently bonded oxygens, N_i, to the total number of oxygens, N, was estimated from the areas corresponding to O 1s photoelectron peaks (Table 1). It was appreciated that around 22 % of oxygen atoms are implied in hydroxyl groups. The oxygen vacancies in the surface layer can act as active sites for H_2O dissociation, producing two hydroxyl-species per dissociated water molecule [25]. The high reactivity of the surface toward water indicates the presence of a large number of O-atoms vacancies [24].

Table 1. The fraction of oxygens in sites of different charge densities.

P (MPa)	600		700			
O 1s BE (eV)	529.95	533.05	529.80	531.10	532.60	535.95
N_i/N (%)	15	85	38	22	12	28

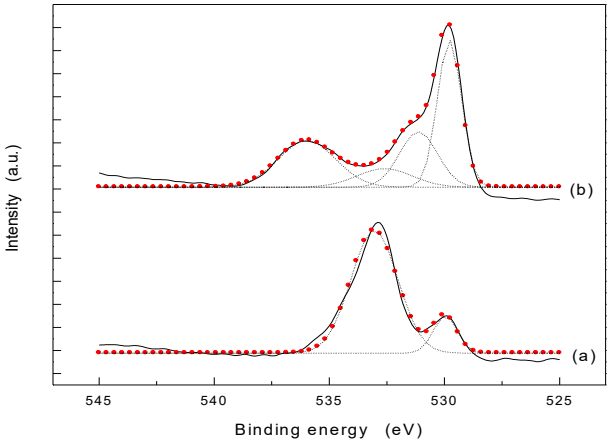

Fig. 4. O 1s core level photoelectron spectra of (a) sample compressed under 600 MPa (b) sample compressed under 700 MPa, experimental (solid line) and fitted (dotted lines) with two, respectivelly four, components (short dot lines).

In the investigated samples the paramagnetic species giving rise to resonance spectra at room temperature are the Fe^{3+} impurities present in titanium powder (0.01%Fe). The EPR spectra (Fig. 5) are dominated by features centred at g = 2.43 for samples pressed at 600 MPa, respectively at g = 2.35 for samples pressed at 700 MPa. In both cases one can recognise the superposition of two lines of different widths (Table 2) arising from Fe^{3+} ions involved in interactions of different strength. The narrow resonance lines arise from iron ions implied in superexchange interactions while the broad lines arise from iron ions mainly implied in dipolar interaction. These lines which are shifted to a lower g value as samples are compresses at a higher pressure and at the same time the narrow line is prevalent upon the broad one, that indicates an increase of the iron ions implied in superexchange interactions in larger iron containing oxide nanocrystals. For the samples compressed at 700 MPa, beside the resonances recorded at g = 2.35 are also recorded two superposed resonance lines centred at g = 3.59 which can be assigned to Fe^{3+} ions disposed in a surrounding perturbed by O^{2-} vacancies [26]. The occurrence of oxygen vacancies is also suggested by Ca 2p and O 1s XPS core level spectra. At the same time, these Fe^{3+} EPR signals could directly indicate changes in the electron configuration of d orbitals of iron ions [27].

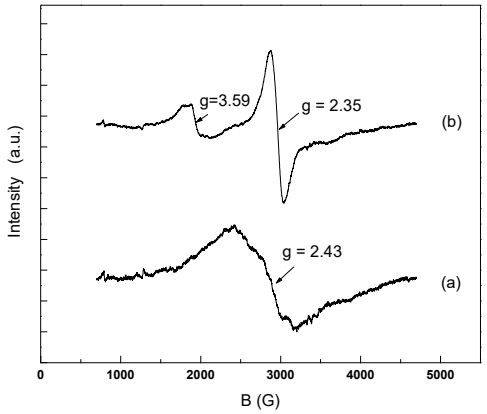

Fig. 4. Fe^{3+} EPR spectra of (a) sample compressed under 600 MPa (b) sample compressed under 700 MPa.

Table 2. Fe^{3+} EPR g factors and line widths.

Pressure (MPa)	g	ΔH (G)
600	2.43	246.7
		799.1
700	2.35	161.3
		1192.9
	3.59	118.5
		332.9

4. Conclusions

Hydroxyapaptite powder with nano-size crystals was used in sintering titanium-hydroxyapaptite samples. In the investigated composites the hydroxyapaptite type phase is strongly distorted. Changes in atomic environment are also determined by increasing the compression pressure from 600 to 700 MPa. The mechanical strain do not affect titanium but leads to new calcium sites with modified electronic properties. Titanium is predominantly involved as Ti^{4+}. The occurrence of O^{2-} vacancies is suggested by Fe^{3+} EPR and O 1s XPS results. Hydroxyl species important for self-assembly of nanoscale hydroxyapatite like structures on endosseous implants are evidenced on the surface of samples compressed at higher pressure.

References

[1] M. T. Pham, M. F. Maitz, W. Matz, H. Reuther, E. Richter, G. Steiner, Thin Solid Films **379**, 50 (2000).
[2] D. A. Cortes, J. C. Escobedo, A. Nogiwa, A. Munoz: Mater. Sci. Forum **442**, 61 (2003).
[3] J. Aboudi, M.-J. Pindera, S. M. Arnold, J. Appl. Mech. **68**, 697 (2001).
[4] D. M. Liu, T. Troczynski, W. J. Tseng, Biomaterials **22**, 172 (2001).
[5] C. Popa, V. Simon, I. Vida-Simiti, G. Batin, V. Candea, S. Simon, J. Mat. Sci.: Mat. in Med. **12**, 1165 (2005).
[6] G. Polzonetti, G. Iucci, A. Frontini, G. Infante, C. Furlani, L. Avigliano, D. Del Principe, G. Palumbo, N. Rosato, Biomaterials **21**, 1531 (2000).
[7] G. Jeschke, H. W. Spiess, in Novel NMR and EPR techniques, eds. J. Dolinsek, M. Vilfan, S. Zumer, Springer Verlag, Berlin, Lect. Notes Phys. **684**, 21 (2006).
[8] JCPDS- International centre for Diffraction Data, 1997, file 21-1272.
[9] Hao Honqi, Wang Yonglan, jin Zhihao, Wang Xiaotian, J. Mat. Sci. **30**, 1233 (1995).
[10] R. Z. Legeros, in: Calcium Phosphates in Oral Biology and Medicine, vol. 15 in Monographs in Oral Science, Ed. H. M. Myers, Karger, Basel 1991, p. 4.
[11] H. P. Klug, L. E. Alexander, X-ray Diffraction Procedures. John Wiley, New York 1954.
[12] R. Sailer, G. McCarthy, JCPDS 44-1294, Int. Centre for Diffraction Data, 1993.
[13] J. W. Wells, G. Cabailhb, D. A. Evans, S. Evans, A. Bushell, A. R. Vearey-Roberts, J. Electron Spectrosc. Rel. Phenom. **141**, 67 (2004).
[14] V. Simon, R. Pop, S. G. Chiuzbaian, M. Neumann, M. Coldea, S. Simon, Mat. Lett. **57**, 2044 (2003).
[15] V. Simon, H. Bako-Szilagyi, M. Neumann, S. G. Chiuzbaian, S. Simon, Mod. Phys. Lett. B, **17**, 291 (2003).
[16] V. Simon, D. Eniu, A. Takács, K. Magyari, M. Neumann, S. Simon, J. Optoelectron. Adv. Mater. **7**, 2853 (2005).
[17] H. T. Cao, Z. L. Pei, J. Gong, C. Sun, R. F. Huang, L. S. Wen, J. Solid State Chem. **177**, 1480 (2004).
[18] K. Cai, A. Rechtenbach, J. Hao, J. Bossert, K. D. Jandt, Biomaterials **26**, 5960-5971 (2005).
[19] T. Albrektsson, M. Jacobsson, J. Prosthet. Dent. **57**, 597 (1987).
[20] H. Chen, B. H. Clarkson, K. Sun, J.F. Mansfield, J. Colloid. Interface Sci. **288**, 97 (2005).
[21] M. T. Pham, W. Matz, H. Reuther, E. Richter, G. Steiner, J. Mat. Sci. Lett. **19**, 1029 (2000).
[22] S. Uhlenbrock, C. Scharfschwert, M. Neumann, G. Illing, H.-J. Freund, J. Phys.: Condens. Matter **4**, 7973 (1992).
[23] H.-J. Freund, H. Kuhlenbeck, M. Neumann, Springer Series in Suface Sciences "Adsorption on Ordered Surfaces of Ionic Solids and Thin Films" **33**, 136 (1993).
[24] M. Kunat, St. Gil Girol, U. Burghaus, Ch. Wöll, J. Phys. Chem. B, **107**, 14350 (2003).
[25] R. Schaub, P. Thostrup, N. Lopez, E. Laegsgaard, I. Stensgaard, K. K. Norskov, F. Besenbacher, Phys. Rev. Lett. **87**, 266104 (2001).
[26] M. Yamaga, T. Yosida, Y. Naitoh, N. Kodama, J. Phys.: Condens. Matter **6**, 4381 (1994).
[27] M. Nakamura, T. Ikeue, H. Fujii, T. Yoshimura, J. Am. Chem. Soc. **119**, 6284 (1997).

*Corresponding author: viosimon@phys.ubbcluj.ro

JOURNAL OF OPTOELECTRONICS AND ADVANCED MATERIALS Vol. 9, No. 3, March 2007, p. 587 - 590